Received: 9 January 2023 | Revised: 26 June 2023 | Accepted: 7 July 2023

DOI: 10.1049/rsn2.12443

IET Radar, Sonar & Navigation

The Institution of Engineering and Technology WILEY

ORIGINAL RESEARCH

Urban traffic congestion alleviation system based on millimeter wave radar and improved probabilistic neural network

Bo Yang[1] | Hua Zhang[1] | Mengxin Du[1] | Anna Wang[2] | Kai Xiong[3]

[1]The School of Aerospace Science and Technology, Xidian University, Xi'an, China

[2]Zhejiang Communications Investment Expressway Construction Management Co., Ltd, Hangzhou, Zhejiang, China

[3]The Beijing Institute of Control Engineering, Beijing, China

Correspondence

Hua Zhang.
Email: zhanghua@mail.xidian.edu.cn

Funding information

Foundation of Science and Technology on Near-Surface Detection Laboratory, Grant/Award Number: 6142414211202; The Basic Research project, Grant/Award Number: 50236170112202; The Civil Aerospace Technology Advanced Research project, Grant/Award Number: D020403

Abstract

The millimeter-wave radar sensor is widely used for urban traffic surveillance because of its weather resistance and high detection accuracy. Methods such as fuzzy theory, pattern recognition, and artificial neural networks have been integrated into the research of traffic state discrimination. However, research on systematically describing the fusion of sensors and traffic state discrimination algorithms to alleviate urban road congestion is still lacking, especially based on millimeter-wave radar. Thus, the authors propose an urban traffic congestion alleviation system framework. First, the design and deployment of the millimeter-wave radar system, including waveforms, signal processing flow, and target tracking, are demonstrated to achieve vehicle information acquisition and output. Then, the appropriate traffic parameters are obtained by analysing traffic state influencing factors and the radar data characteristics. Finally, a traffic conditions identification algorithm combining spectral clustering and neural network algorithm is presented to realise road congestion level classification. The system is applied to real urban intersections rather than simulation or approximate real simulation. According to the current road congestion level, regulate the traffic light state to achieve road vehicle driving command. Experiments show that the proposed system can effectively reduce road congestion by 20% compared to the current fixed traffic light system.

KEYWORDS

millimeter wave radar, neural nets, road traffic

1 | INTRODUCTION

The conflict between the growth in the number of vehicles and the limited lane capacity has led to traffic congestion, especially during peak hours. The economic losses [1] and road safety risks associated with traffic congestion force people to find solutions. Using historical traffic information data to establish a macro-control model is a typical method of achieving urban traffic flow management and congestion prediction. For example, in Ref. [2], a residual graph convolution long short-term memory model is proposed to predict short-term traffic on urban networks with more accurate predictions during peak periods than traditional statistical models [3–5] and machine learning models [6–8]. However, handling emergencies (extreme antennas and accidents) still requires further research due to the lack of real-time. In addition, the prediction accuracy is also limited by the spatial span of the urban road network.

Aiming at the changeable and uncontrollable characteristics of urban traffic roads, a new traffic management method based on real-time vehicle information at the current intersection node is proposed. The sensors installed on the roadside collect vehicle information and then send the vehicle parameters to the edge computer for processing to obtain the current road congestion status and finally adjust the traffic light status according to the road status to realise vehicle driving management. Utilising real-time data rather than historical or expected traffic flow data is the biggest advantage of this approach. Now, implementing traffic commands based on on-road vehicle information from traffic sensors is considered the most likely means of solving traffic congestion and avoiding traffic accidents, which is the need for intelligent transportation development [9–11]. In particular, the accuracy and characteristics of traffic sensors directly affect the accuracy and efficiency of congestion mitigation and are therefore widely studied.

1.1 | Traffic sensor development and millimeter wave radar features

Magnetometer (MAG) sensors are used for traffic monitoring because they are sensitive and inexpensive [12]. With the maturity of wireless sensor (WSN) technology, the integration of MAG and WSN has enabled the detection of road vehicle speed estimation, vehicle classification, and traffic monitoring [13, 14]. However, MAG can be affected by vehicle size, vehicle structure, and density. More importantly, having to rely on the vehicle to pass to perform detection limits the sensor's ability to sense road information.

Video cameras are currently the most widely used sensing system in traffic surveillance due to their ability to visually provide image information. Researchers have proposed improved methods based on vehicle monitoring systems with conventional vision systems. A surveillance system using multiple camera devices is networked [15, 16] to improve vehicle monitoring and management in urban intersection areas. A deep learning network based on video data is proposed to achieve road congestion classification and regulation [17]. Traffic congestion mitigation is implemented using road uncalibrated camera systems for vehicle speed and flow estimation based on digital image processing techniques [18]. And multi-sensor fusion techniques such as video and LIDAR fusion are proposed to achieve road congestion discrimination [19]. However, the camera does not directly access distance information and is susceptible to light and weather. Although the current night vision function is added to the camera, it also increases the cost [20].

Frequency modulated continuous wave (FMCW) millimeter wave radar has received much attention since its birth due to its high range resolution, high-velocity resolution, and environmental robustness. The research on radar constant false alarm detection techniques [21–23] and radar beams [24] improves radar multi-target detection ability. And some technologies are presented to enhance radar velocity detection range, such as proposing Binary Phase Modulation technology [25] for improving radar maximum unambiguous velocity detection and using the Inverse Synthetic Aperture Radar algorithms [26] to improve radar detection of slow targets. These studies make the millimeter-wave radar more suitable for urban road traffic environments.

1.2 | Millimeter wave radar-based road application and congestion alleviation system research

Some high-resolution or improved radar systems are designed to implement vehicle speed and type detection in traffic scenes [27] or radial and tangential speed detection of multi-lane vehicles [28]. Interferometric linear continuous wave is proposed to implement vehicle detection on highways [29], and slow time direction Fourier transform is used to implement slow-moving vehicle detection [30]. Research radar multi-frame data or micro-Doppler features of targets achieve road vehicle length detection [31] or type identification [32] and designing a non-contact millimeter-wave radar system [33] or installing millimeter-wave radar on top of the road [34] for road traffic flow detection.

As aforementioned, radar sensors still play a "surveillance" role. Few studies have participated in traffic command to improve road traffic congestion. In Ref. [35], a new method for calculating intersection phase time series based on interval detection data from millimeter-wave radars reduces vehicle congestion at intersections. And some systems based on the fusion of millimeter-wave radar and camera have been proposed to improve the robustness of vehicle information awareness on urban roads [36, 37]. However, these studies based on the millimeter-wave radar to achieve traffic congestion relief are presented in simulation or approximate real simulation. In addition, the design description of the millimeter wave radar system applied to traffic congestion management is relatively rough.

1.3 | Traffic status recognition technology research

Traffic status recognition techniques have been developed in recent years. Fuzzy theory, pattern recognition, and artificial neural networks have been applied to traffic discrimination research. For example, adaptive fuzzy logic neural networks are trained to learn to discriminate traffic states based on congestion values given by the subjective evaluations of simulated traffic flows. Cluster analysis is an unsupervised learning algorithm, including coalescent clustering algorithm [38], Fuzzy C Means Clustering (FCM) algorithm [39, 40], and K-means clustering algorithm [41]. It can classify data without any reference, which is especially suitable for traffic flow data with complex data association, where the K-means clustering algorithm (K-means) can achieve 87% traffic congestion recognition rate [42]. Supervised algorithms, including Radial Basis Function (RBF) neural networks [43], Back Propagation Neural Network [44], Probabilistic Neural Network (PNN) [45], and Optimisation SVM [46] also have good traffic congestion discriminatory effects. Other scholars have combined unsupervised algorithms with supervised ones, for example, mixing K-means and multi-classification SVM [47], which improve the accuracy and have good robustness.

1.4 | Article contribution

As aforementioned, using millimeter-wave radar and road traffic discrimination algorithms is a feasible way to achieve road traffic congestion relief. However, there is little research on the integration of millimeter-wave radar systems with traffic discrimination techniques to give a complete road congestion mitigation system. In addition, most of the studies based on the millimeter-wave radar to achieve traffic congestion relief are presented in simulation or approximate real simulation, and the system description is rough. To make up for the weaknesses in the research field and reduce urban congestion and promote the development of radar system applications, we propose an urban traffic congestion alleviation system based on millimeter wave radar and improved PNN. The system directs vehicle movements by controlling traffic lights at intersections to achieve traffic congestion relief. The contributions of this paper are summarised as follows:

- This paper describes in detail the framework and design process of the traffic congestion mitigation system. The system closely integrates the research of millimeter wave radar research, neural network-based traffic condition discrimination techniques, and traffic signal control to alleviate congestion at urban intersections.
- The key aspects and design ideas of the urban traffic congestion alleviation system are presented and described in detail, covering the entire spectrum from mmWave radar design and traffic parameters analysis to the development of a traffic conditions identification algorithm.
- In designing and elaborating the key links of the traffic congestion mitigation system, the article also proposes some new algorithms (e.g., Monte Carlo-based constant false alarm detection algorithm (the MC-CFAR), improved probabilistic neural network algorithm (the SC-PNN), etc.) for reference, hoping to shorten the development cycle of researchers.
- Different from the simulation system or approximate simulation system, the proposed urban road congestion alleviation system has been applied to urban intersections with initial success. The system was implemented at No. 191, Changshan Road, Laiyang City, Yantai City, Shandong Province, China. After 2 months of testing, it effectively reduced traffic congestion by more than 20% compared to fixed-hour traffic light systems.

The structure of this paper is organised as follows. Section 2 analyses a typical urban intersection environment and gives an overview of the traffic congestion alleviation system. In Sections 3–5, the design process of each part of the traffic congestion mitigation system is elaborated. After that, in Section 6, traffic congestion system application effects are investigated. Finally, Section 7 summarises the conclusions of this paper and future works.

2 | TRAFFIC SCENARIO ANALYSIS AND TRAFFIC CONGESTION ALLEVIATION SYSTEM OVERVIEW

2.1 | Traffic scenario

Traffic intersections are an essential part of a city. The traffic light system installed at the intersection directs vehicles to pass through the state of the light signal. These signal light state durations are usually set based on historical intersection traffic data and are almost constant over a period of time. However, the traffic conditions are complex and dynamic, so the fixed-time traffic light command system cannot be flexibly adjusted according to the current road conditions, making intersections the city's most frequent congestion areas.

Intuitive vehicle driving information (e.g., vehicle speed, vehicle location, and vehicle queue length) and non-intuitive road state information (average road speed and traffic flow) make up the traffic parameters, which reflect the congestion level of the road, as shown in Figure 1. Therefore, a road congestion alleviation system is needed: Real-time analysis of road information from traffic sensor data to perceive road congestion level purposefully control the intersection traffic light duration to direct vehicles to wait or release to reduce traffic congestion, improve road utilisation, and ensure smooth road flow.

2.2 | Traffic congestion alleviation system architecture and system deployment

Figure 2 shows an overview of the proposed traffic congestion alleviation system. The front-end millimeter-wave radar system monitors road vehicles in real time and provides road vehicle information for the back-end traffic state recognition system through radar detection and radar tracking processing. The back-end traffic conditions identification system obtains the road congestion level and gives traffic light control decisions by processing vehicle information from the radar system. The traffic parameter extraction unit receives the vehicle information output by the radar and outputs traffic parameters, including traffic flow, queue length, average road speed. Then the proposed improved PNN algorithm gives the current road congestion level by processing the traffic parameters. The traffic light control system adjusts the duration of the light signal according to the current road congestion level to achieve the relief of road traffic congestion.

In practical applications, a complete traffic congestion alleviation system consists of multiple front-end radar systems and a back-end traffic conditions identification system. As shown in Figure 3, in a traffic intersection environment, four front-end radar systems are installed on the four traffic light brackets respectively at the traffic intersection and face the

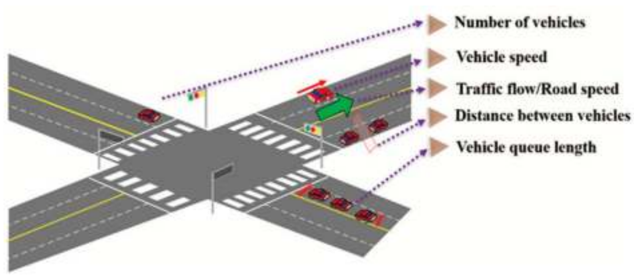

FIGURE 1 Traffic intersection scene.

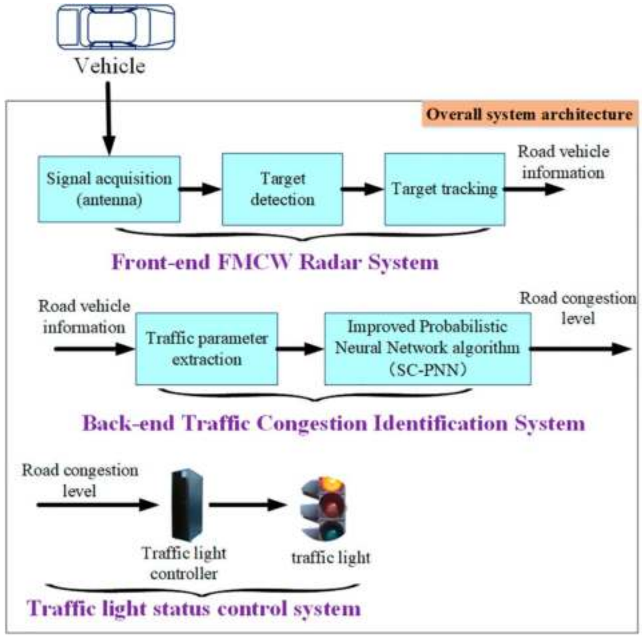

FIGURE 2 Traffic congestion alleviation system overall architecture.

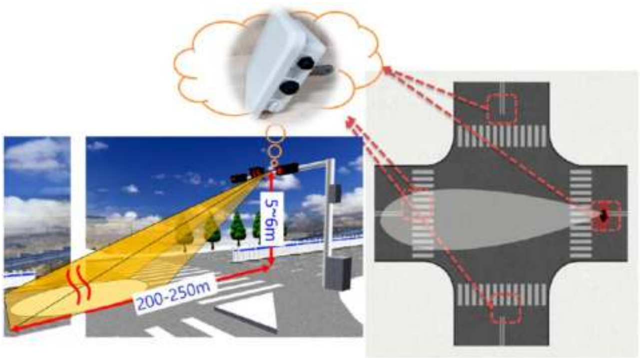

FIGURE 3 Traffic congestion alleviation system deployment method diagram.

opposite side of the lane to achieve full coverage of the entire traffic intersection area. The traffic status discrimination system receives all radar system data, performs data processing and state judgment, and transmits the decision information to the edge computer, where the traffic light is located to control the state of the traffic light.

3 | MILLIMETER WAVE RADAR DESIGN AND KEY TECHNOLOGIES COMPARATIVE ANALYSIS

Traffic sensors, as the eye of the urban road surveillance systems, play an essential role in the whole system. This chapter presents the proposed millimeter-wave radar system design with the system architecture, as shown in Figure 4 and compare and analyse the key technologies. The main points are as follows:

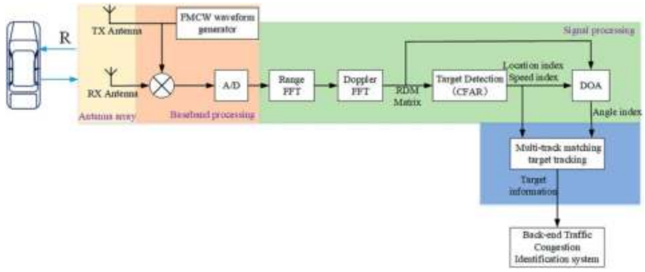

FIGURE 4 Front-end Frequency modulated continuous wave (FMCW) radar system architecture.

- Radar system hardware platform and beam design.
- Radar signal processing process design for vehicle information acquisition.
- A multi-track matching target tracking algorithm design to improve target surveillance continuity and remove false target interference.

3.1 | Radar system hardware platform and beam design

To analyse the city road surveillance, we collect vehicle data through a self-designed millimeter-wave radar system whose composition is shown in Figure 5a. The four radar chips cascade (AWR2243) based Radio Frequency (RF) front-end with 12 transmitting and 16 receiving antennas is used to transmit millimeter-wave and receive target echo signals. Additionally, sixteen-channel high-speed ADC is used for vehicle raw data acquisition. And raw data is sent to the baseband processing system via a high-speed interface. Figure 5b shows the radar baseband processing platform, and we use the physical architecture of FPGA + RAM to provide a platform for software development. At the same time, six pieces of DDR memory (two on the FPGA side and four on the RAM side) are used to support the data processing and data flow of the algorithm. Finally, vehicle information such as location, speed, and bearing information is transmitted through the network port.

The radar transmitting beam is designed based on the urban 4-lane road as the basic surveillance unit to achieve road area coverage. As shown in Figure 6, the red line indicates the antenna azimuth beam map with a maximum gain 21 dB, 12 degrees of 3 dB beamwidth and 20 degrees of 8 dB beamwidth. And the green line is the elevation beam map and has the same parameters as the azimuth beam map. In addition, the phased array approach is used to change the radar beam pointing, that is, expand the radar surveillance range by beam scanning to adapt to the surveillance of the intersections with more lanes (e.g., six or eight lanes).

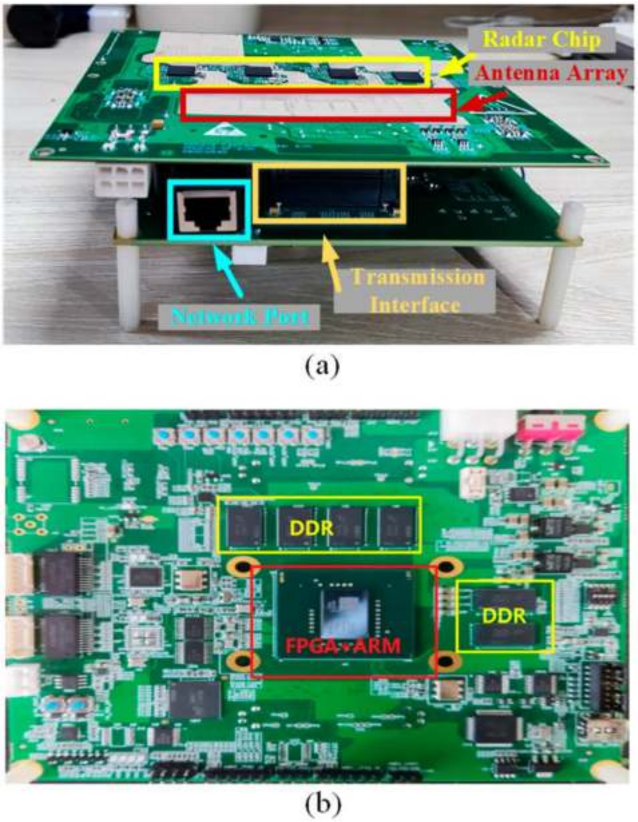

FIGURE 5 Front-end Frequency modulated continuous wave (FMCW) radar system hardware architecture. (a) Radar RF board and data transmission interface. (b) Radar baseband signal processing board.

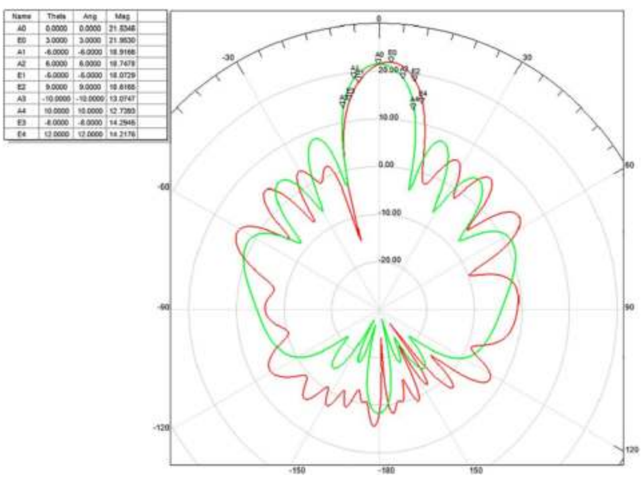

FIGURE 6 Front-end radar system transmitting antenna beam pattern.

3.2 | Radar signal processing flow design

3.2.1 | Millimeter-wave radar target detection principle

Millimeter-wave radar obtains target information by collecting target echo signals. The radar transmits the chirp signal (TX) and captures its transmission path's object reflection signal (RX). The RX signal is the same as the TX signal but lags by τ which is the propagation time of the waveform between the radar and the object. The mixer mixes the RX signal and the current TX signal to obtain an intermediate frequency signal, also called beat frequency signal (f_b). The frequency value of the f_b reflects the distance of the target from the radar. The relationship between the target distance and the intermediate frequency is

$$R = \frac{c\tau}{2} = \frac{cf_b}{2K} = \frac{cf_bT_c}{2B} \tag{1}$$

where R represents the distance between the radar and the target; c represents the speed of light; T_c represents the Chirp cycle; and B is the bandwidth.

To measure the speed, the radar transmits at least two chirp pulses with a time interval of T_c. Because the electromagnetic wave can be considered as $f_o \gg B$, so the phase difference $\Delta\phi$ caused by the movement of the object can be expressed as

$$\Delta\phi = 2\pi f_o t = \frac{4\pi f_o \Delta R}{c} = \frac{4\pi v T_c}{\lambda} \tag{2}$$

where ΔR represents the displacement of the object in time t; λ represents the wavelength; v represents the speed of the target. The relationship between the phase difference and Doppler within T_c is

$$\Delta\phi = 2\pi f_d T_c \tag{3}$$

where f_d represents the Doppler at velocity v. So combining formula (2) and formula (3), the relationship between velocity and Doppler is

$$f_d = \frac{2v}{\lambda} \tag{4}$$

In a radar system, at least two receiving antennas are required to realise the estimation of the target azimuth angle. Suppose the receiving antenna is uniformly distributed, the distance between the antennas is d, and the angle between the target and the radar is θ. The signal propagation distance difference between RX antennas is $dsin(\theta)$ from the geometric relationship. Therefore, the phase difference ($\Delta\omega$) between adjacent receiving antennas is

$$\Delta\omega = (2\pi/\lambda)dsin(\theta) \tag{5}$$

Then the angle of arrival of the object can be expressed as

$$\theta = \arcsin\left(\frac{\Delta\omega\lambda}{2\pi d}\right) \tag{6}$$

In practical application, we can obtain the parameters (f_b, f_d, and $\Delta\omega$) by performing FFT operations and detection algorithm.

3.2.2 | 2D FFT processing

In FMCW radar systems, the transmit signal is a single tone with a linear change in frequency over time called "chirp". Target distance is obtained by processing a chirp signal, and target velocity is obtained by transmitting and processing multiple chirp signals with the same parameters.

Our sampling and FFT processing of a single chirp is called radar fast time dimension processing (i.e., Range-FFT). Next, multiple chirp sequence data are stacked and FFT processing on the same distance unit, called radar slow time processing (i.e., Doppler-FFT). The two FFT processing on the distance and velocity dimensions are called two-dimensional FFT (2D-FFT).

In the same period, each one of the channels generates a Range-Doppler Matrix (RDM) containing target distance and velocity information with the same scale size by 2D-FFT processing.

3.2.3 | Radar CFAR detection

The radar CFAR detection technologies separate the target and the background noise in the RDM matrix by setting the threshold according to different clutter environments [48]. Currently, commonly used CFAR algorithms include Cell Averaging CFAR (CA-CFAR) [49], Ordered Statistical CFAR (OS-CFAR) [50]. The CA-CFRA algorithm has low CFAR loss but cannot be used for multi-target detection, and the OS-CFAR algorithm has good multi-target detection capabilities but has a large CFAR loss.

In previous work, we proposed a Monte Carlo random sampling-based CFAR detection algorithm (MC-CFAR) [51] for vehicle detection in the road traffic environment, which estimates the background noise where the moving target is located by randomly sampling the RDM, as shown in Figure 7. The performance comparison of the algorithm is shown in Figure 8. Compared with the conventional CFAR detection algorithm, the proposed detection algorithm has higher detection sensitivity and lower algorithmic complexity. More importantly, the algorithm avoids reference window sliding, which greatly reduces the radar signal processing latency and improves the system's real-time performance.

Each cell $X_{m,n}$ of the synthesis matrix represents the distance and velocity of the target, where m represents the target distance index and n represents the target speed index. The distance and velocity information of the target is outputted by CFAR detector processing.

3.2.4 | Target angle finding

There are many methods for target angle search, the most typical ones are multiple signal classification algorithm [52] and rational invariance techniques (ESPRIT) algorithm [53], but these angle estimation methods rely on the accurate estimation of the array covariance matrix with multiple snapshots. To find the target angle with one snapshot, the orthogonal matching pursuit algorithm [54] and the iterative adaptive approach algorithm [55] are proposed; however, they have a high computational cost. The digital beamforming (DBF) [56] is a method to obtain the target angle values by power spectrum peak search. Although the accuracy is relatively poor, it is easy to implement and requires only one snapshot. Taking into account, the DBF method is selected for target angle discovery in this system.

3.3 | Multi-track matching target tracking algorithm

The target information points obtained by the radar signal processing part are not directly fed to the back-end traffic state resolution system. The reasons are as follows:

- There are false targets due to false alarms of the CFAR detector and external interference. And it is not conducive to the statistics of the number of vehicles
- The target information obtained by signal processing has poor stability and requires filtering and smoothing.

We use multi-track matching target tracking architecture (as shown in Figure 9) to achieve stable monitoring and tracking of road vehicles, provide stable vehicle travel information for the road congestion identification system, and ensure the accuracy

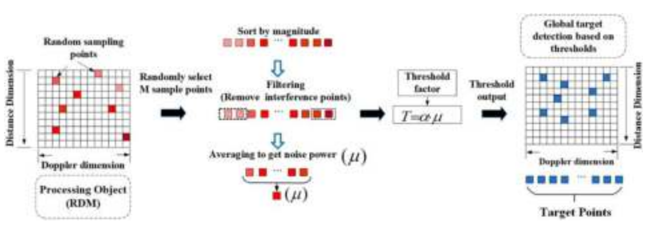

FIGURE 7 Front-end radar system target detection algorithm (the MC-CFAR) process.

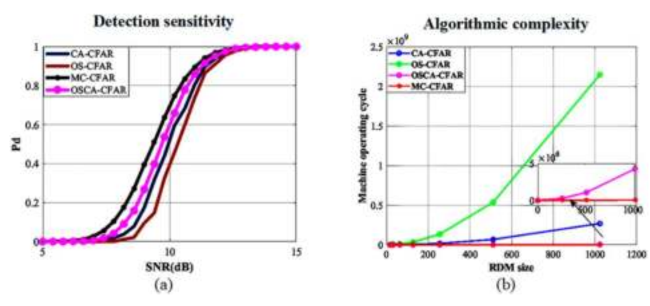

FIGURE 8 The MC-CFAR algorithm performance. (a) Detection sensitivity comparison. (b) Computational complexity comparison.

of road status discrimination. The tracking system processes the vehicle target data from the radar signal processing section at frame time intervals. At any moment, the system has three types of target trajectories set, such as starting trajectory set, temporary trajectory set, and reliable trajectory set. Through the operations of coordinate transformation, trajectory matching, filtering, prediction, and trajectory iteration, the vehicle information in the reliable trajectory is finally outputted .

3.3.1 | Vehicle target coordinate conversion

The radar signal processing part transmits the set of all target information in the current radar field of view in time units of frames, which can be represented as

$$A = \{a_1, a_2, \ldots, a_n | a_i = \{R_{i,adar}, V_{i,adar}, \theta_{i,adar}\}\} \tag{7}$$

where A represents the set of all target points in a frame; a_i is a subset of A, which means the target point, and $i = 1, 2, \ldots, n$; $R_{i,adar}, V_{i,adar}, \theta_{i,adar}$ respectively, represent the distance, speed and angle information of the ith target point relative to the radar.

According to the geometric relationship between the radar and the target, as shown in Figure 10, we can get the position and speed information of the target on the road. So the position of the vehicle in the lane is:

$$\begin{cases} x_{i\_car} = R_i \cos|\theta_i|, y_{i\_car} = -R_i \cos|\theta_i| & \theta_i < 0 \\ x_{i\_car} = R_i \sin|\theta_i|, y_{i\_car} = +R_i \sin|\theta_i| & \theta_i > 0 \end{cases} \tag{8}$$

where x_{i_car}, y_{i_car} are the road coordinates of the ith vehicle; R_i is the distance between the origin of the coordinates and the ith target, $R_i = \sqrt{R_{i\_radar}^2 - h_r^2}$; Similarly, we can obtain the true speed of the target:

$$\begin{cases} V_{i\_car}^{y} = V_{i,adar} \cos|\theta_i| \\ V_{i\_car}^{x} = V_{i,adar} \sin|\theta_i| \end{cases} \tag{9}$$

where $V_{i\_car}^{y}$ and $V_{i\_car}^{x}$ respectively represent the radial velocity and lateral velocity of the target, and $V_i = V_{i\_radar} \cos\vartheta$. Then the target point set from the signal processing part is transformed into set B:

$$B = \{b_1, b_2, \ldots, b_n | b_i = \{R_{i\_car}, V_{i\_car}, \theta_{i\_car}\}\} \tag{10}$$

where b_i is a subset of B, which represents the actual information of the ith target on the road.

3.3.2 | Trajectory matching

The purpose of track matching is to divide each vehicle information into the corresponding vehicle tracks, and the division principle is as follows:

- First, each vehicle information point is matched with each existing trajectory in turn. There is a predicted value (called vehicle information prediction point) in each already existing vehicle trajectory, and the current vehicle information point is matched with this expected value. Once the matching is successful, the vehicle information point is considered to belong to this trajectory and will not be matched with other trajectories.
- When multiple vehicle information points meet the matching requirements, the filtering is performed with the closest criterion. And the rest of the points will be discarded.
- Finally, the remaining vehicle information points that do not belong to any of the tracks will be used as new track start points in the starting trajectory unit for track start, respectively

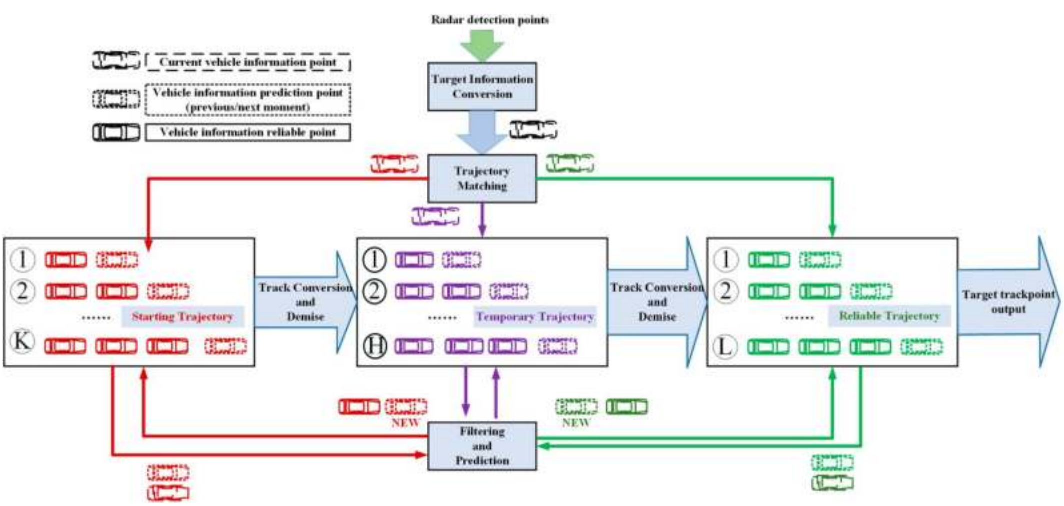

FIGURE 9 Front-end radar system target tracking process.

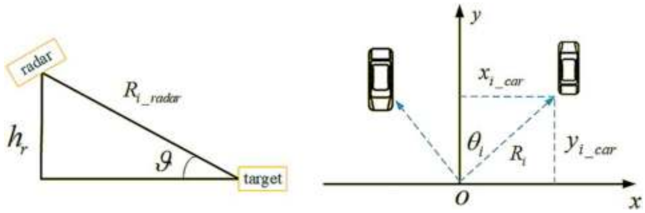

FIGURE 10 The geometric relationship between radar and target.

3.3.3 | Filtering and prediction

The Kalman Filter algorithm (KF), which is a linear filter with good performance when the noise process is Gaussian, is used to realise the filtering and prediction of the track. Considering that the target speed varies with the actual situation, we use the Constant Acceleration as the KF system model:

$$\begin{cases} x_{k+1} = x_k + \dot{x}_k T + \frac{1}{2}\ddot{x}_k T^2 \\ y_{k+1} = y_k + \dot{y}_k T + \frac{1}{2}\ddot{y}_k T^2 \\ \dot{x_{k+1}} = \dot{x}_k + \ddot{x}_k T \\ \dot{y_{k+1}} = \dot{y}_k + \ddot{y}_k T \\ \ddot{x_{k+1}} = \ddot{x}_k \\ \ddot{y_{k+1}} = \ddot{y}_k \end{cases} \tag{11}$$

where x, $\dot{x}$, and y, $\dot{y}$ represent the position and velocity of the target in the x-axis and y-axis directions; $\ddot{x}$ and$\ddot{y}$ are the acceleration; T is the observation period. The predicted value of the tracks and the current vehicle information point that best matches this track at the current time are sent to the KF system model for processing. Then, the filtered value (new vehicle information reliable value) is used for trajectory update and output, and the new predicted value is used for trajectory matching at the next moment.

Through Kalman filtering and prediction algorithms, the messy target information points are transformed into stable and continuous track points. Each trajectory in the three trajectory units is updated and processed the same way. Still, the only difference is that the reliable track points after Kalman filtering will be outputted to the traffic conditions identification system as the data source.

3.3.4 | Track conversion and demise

The conversion of the target trajectory type is unidirectional, and each vehicle trajectory is assigned a separate counter that records how often that track is updated. As the accumulated value of the counter rises steadily, the more reliable this vehicle trajectory becomes. This vehicle track is gradually transferred from the initial starting trajectory unit to the reliable trajectory unit with increasing reliability. The vehicle trajectory in the reliable trajectory unit has the highest reliability, that is, there exists a vehicle corresponding to that track driving in the radar view.

In the starting and temporary trajectory units, once the counter corresponding to the vehicle trajectory stops accumulating and the stop time exceeds the threshold, it is directly determined that the trajectory is dead. For the vehicle trajectory in the reliable trajectory unit, before judging the dead of the trajectory, it is necessary to judge whether the vehicle disappears or stops according to the position of the vehicle. When the vehicle disappears from the radar field of view, the vehicle trajectory is eliminated. If the vehicle stops, the track of the vehicle is preserved.

3.3.5 | Target trajectory points output

In the reliable trajectory unit, each track's latest target trajectory points are output to the state discrimination system at 50 Hz, which includes the vehicle speed, position, and lane.

3.4 | Radar performance test

We verify the performance of the proposed radar system by observing the tracking effect of the radar on-road vehicles. Theoretically, the better the effect of radar on vehicle target tracking, the more accurate the congestion mitigation system will be in identifying road congestion levels.

Figure 11 shows the tracking effect of the radar system on vehicles. Before tracking, the original detection points of the radar to the vehicle target are cluttered and have many interference points (as shown in Figure 11a). It cannot accurately determine the trajectory of the vehicle and the vehicle's number. Figure 11b shows the result of radar tracking processing. We use different slopes to represent the direction of the vehicle and different colors to represent different vehicle trajectories. After the tracking process, the false target is eliminated, and the target point is more continuous, concentrated, and stable. Figure 12 shows the tracking accuracy of the radar system on vehicles at different distances (the maximum detection range of the radar is 200 m). Through statistics, the tracking accuracy of vehicles in the entire road section is greater than 85%.

4 | TRAFFIC PARAMETERS SELECTION

Selecting appropriate traffic parameters helps improve the identification efficiency and accuracy and reduces the identification algorithm's complexity. Usually, the selection of traffic feature parameters should follow intuitiveness, systematicness, convenience, and suitability. Considering the characteristics of radar data (easy-to-obtain target speed and distance information)

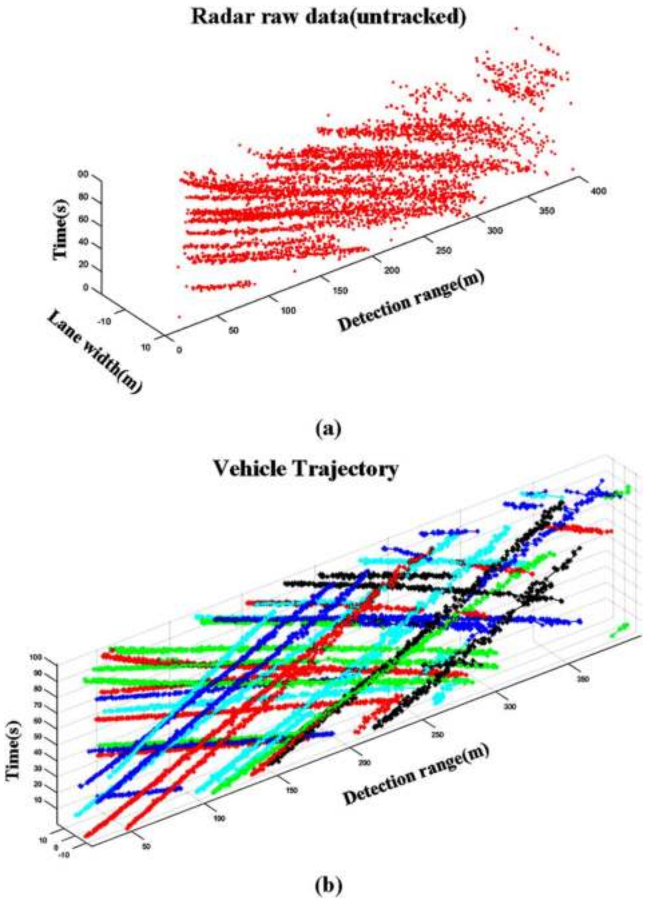

FIGURE 11 Front-end radar system tracking functional testing. (a) Radar raw data. (b) Radar tracking results.

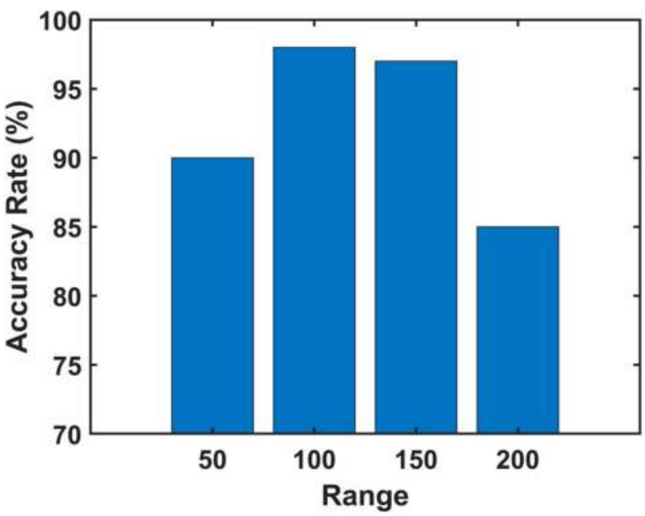

FIGURE 12 Front-end Radar system vehicle tracking performance statistics results.

and traffic intersection environment (vehicles increase during the waiting time for traffic lights), we choose three traffic parameters, the average road speed, traffic flow, and vehicle queuing length as the basis for traffic state identification.

4.1 | Parameter extraction of average road speed

The common method is to directly add up all target speeds per unit of time and average them to obtain the average road speed, but this method has errors since the vehicle cannot keep driving at a constant speed at an intersection. To get an accurate average road speed, we obtain the average speed of each vehicle in a period and then obtain the average road speed by averaging the average speed of all vehicles. The operation process is as follows:

- Step 1: Obtain all vehicle's speed data from radar in a fixed time period.
- Step 2: Calculate the average speed of each car in this period of time:

$$v_i = \frac{\sum_{j=1}^{n} v_{ij}}{n}, i = 1, 2, \ldots, n \tag{12}$$

where v_{ij} represents the speed of each track point of the ith vehicle, and n represents the number of vehicles in the time period.

- Step 3: We calculate the average speed of each vehicle obtained in step 2 to obtain the average road speed:

$$v_{road} = \frac{\sum_{i=1}^{m}}{m} \tag{13}$$

where v_i is the average speed of each vehicle obtained in step 2; n is the number of vehicles, which is obtained through the flow calculation model.

4.2 | Parameter extraction of traffic flow

The traffic flow reflects the current traffic load on the road. When traffic exceeds a certain limit, congestion will generally occur. In a radar system, the number of tracks in the reliable track unit directly reflects the number of vehicles on the road at that moment. Moreover, in the vehicle information output by the radar, each vehicle has its unique ID number. Thus, we can obtain road traffic flow by counting the number of IDs:

- Step 1: Obtain all the vehicle "ID" numbers in the time period.
- Step 2: Remove the records with the same vehicle "ID" and only keep one "ID" record.
- Step 3: Count the number of "ID" of different vehicles to get the number of traffic flows during the time.

4.3 | Parameter extraction of vehicle queue length

The queuing length refers to the length of vehicles that line up head to tail. When congestion occurs, the size of the vehicle queue will increase, so the size of the queue can more intuitively reflect the road congestion.

Based on the radar detection data, a method for estimating the length of the online queue at an intersection is proposed. The key of the method is to divide the road into several cells and count the number of cells with continuous vehicle information to estimate the length of the queue. The road length estimation model is shown in Figure 13, and the specific principles are as follows:

- Step 1: Divide the road into several lanes according to the actual situation, and divide lanes into several cells similar to the length of the vehicle, and count whether there is vehicle information in each cell per unit of time.
- Step 2: Taking into account the influence of factors such as the safety distance of the vehicle and the driver, if the vehicle information is missing in two consecutive cells, it is considered to have reached the end of the fleet.
- Step 3: A complete fleet comprises consecutive cells with no more than two consecutive cells with missing vehicle data. And the queue length value is the product of the number of cells in this queue and the length of a single cell.
- Step 4: In the end, select the maximum lane queue length as the road queue length.

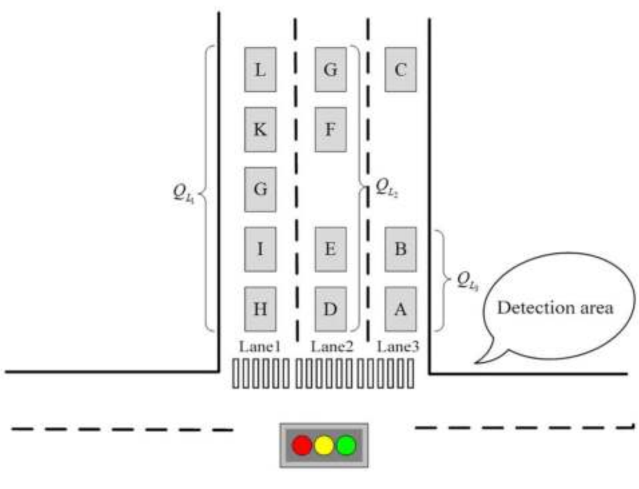

FIGURE 13 Schematic diagram of road queue length estimation.

5 | TRAFFIC CONDITION IDENTIFICATION BASED ON SC-PNN ALGORITHM

Traffic state discrimination methods are mainly divided into two categories: unsupervised algorithms and supervised algorithms. As a typical unsupervised algorithm, the clustering algorithm can be classified according to the similarity between data without any reference, which is in line with the research of traffic data. Still, due to the computational complexity, the real-time performance of the algorithm cannot be guaranteed. The supervised algorithm overcomes the real-time problem of the unsupervised algorithm. Still, it cannot directly discover the classification rules by itself and needs the assistance of a dataset with classification labels. Therefore, a combination of unsupervised and supervised algorithms ensures real-time discrimination while providing classification information.

5.1 | Determination of the classification number of traffic states

There are differences in the scale and road level between different countries and cities, making the evaluation criteria of traffic status various. Since the data selected for state discrimination in this study are traffic flow, average road speed, and queue length, there is no classification label. Therefore, the internal evaluation standard of the clustering algorithm is adopted, that is, the silhouette coefficient is used to determine the number of state classifications.

The silhouette Coefficient is an evaluation method of the clustering effect, and its expression is

$$sc = \frac{b - a}{\max(a, b)} \tag{14}$$

where sc represents the silhouette coefficient of each sample; a is the average distance between the data and other data of the same class; b is the average distance between the data and all points of the similar class. The silhouette coefficient takes values between −1 and one, with a higher score when the data is dense and well separated. A value of zero indicates that the data is very close to the decision boundary of two adjacent clusters. In contrast, a value less than zero indicates that it may have been classified into the wrong category.

Table 1 shows the average score of the silhouette coefficient when the number of categories is [2, 7]. The effect is best when the number of classifications is set to five. So the data is divided into five categories. The corresponding traffic status is very smooth, smooth, mild congestion, congestion, and severe congestion.

TABLE 1 The relationship between the number of classifications and the average silhouette coefficient score.

Number of classifications	Average silhouette coefficient score
2	0.52
3	0.53
4	0.54
5	0.69
6	0.41
7	0.42

5.2 | The SC-PNN algorithm principle and implementation steps

5.2.1 | Spectral clustering algorithm principle

Spectral Clustering (SC) is a new unsupervised clustering algorithm that transforms the sample clustering problem into a graph and divides the data using knowledge from graph theory to achieve a high similarity between similar classes and low similarity between different categories. The SC algorithm has the advantages of low computational complexity, not being limited by the shape of the sample space and strong adaptability to data distribution. The algorithm flow is as follows:

- Step 1: Generate a similarity matrix S based on the input traffic parameter dataset.
- Step 2: Construct adjacency matrix W and degree matrix D from the similarity matrix S.
- Step 3: Calculate the Laplacian matrix L from the W matrix and the D matrix.
- Step 4: Construct the normalised Laplacian matrix $D^{-\frac{1}{2}}LD^{-\frac{1}{2}}$.
- Step 5: Perform a clustering operation on the feature matrix according to the k-means algorithm.
- Step 6: Get the results of cluster division: very smooth, smooth, mild congested, congested, and severe congested.

5.2.2 | Probabilistic neural network algorithm

The PNN algorithm is a radial basis neural network with a simple structure, good fault tolerance, accurate classification, fast training speed, and can discriminate traffic status in real-time. Figure 14 shows the structure of the PNN. And the algorithm flow is as follows:

- Step 1: Normalise the input training dataset and test dataset.
- Step 2: Send the normalised sample data into the input layer of the network.
- Step 3: Calculate the Euclidean distance between the test dataset and the training dataset.
- Step 4: Get the initial probability based on the Gaussian function.
- Step 5: Get category probabilities by summing the probabilities.
- Step 6: Output the category with the highest probability.

5.2.3 | SC-PNN algorithm principle

The SC algorithm gets the similarity matrix from a large amount of data for classification, suitable for traffic state discrimination. However, if the clustering dimension is very high, the running speed of the algorithm and the final clustering effect will be affected due to insufficient dimensionality reduction. Meanwhile, the clustering effect has a great correlation with the similarity matrix, and the selection of the similarity matrix also affects the clustering effect of the data. Therefore, the PNN algorithm of the supervised learning algorithm is chosen for training and testing the clustering results to improve the accuracy of the results and make the classification more accurate.

We propose a traffic identification algorithm based on SC and PNN (as shown in Figure 15). Firstly, the SC algorithm is used to classify the processed traffic flow data, and then the PNN algorithm is used to train the classified data and labels. This method enhances classification accuracy and improves the speed of discrimination and the real-time performance of data processing, which meets traffic control needs.

- Step 1: Traffic parameters input, including traffic flow, average road speed, and queue length.
- Step 2: The SC algorithm determines the divided traffic states: very smooth, smooth, mild congested, congested, and severe congested.

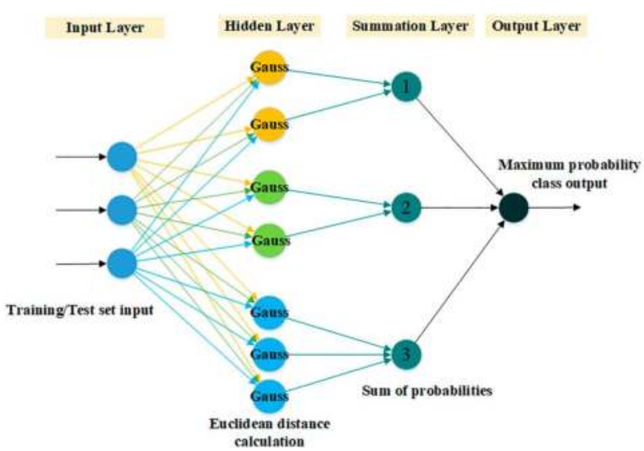

FIGURE 14 The structure of the probabilistic neural network (PNN).

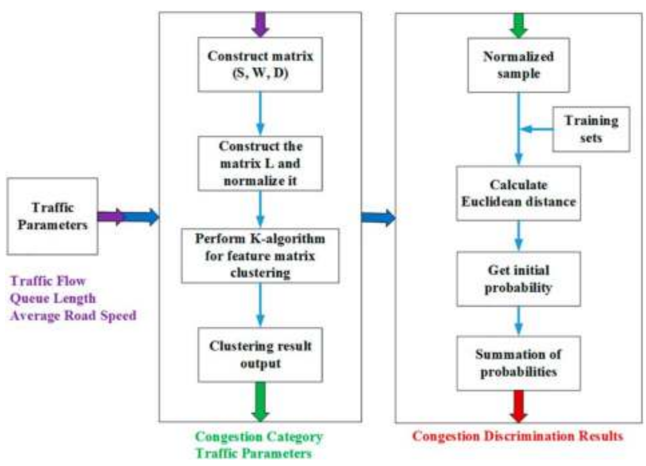

FIGURE 15 Traffic congestion state identification algorithm (the SC-PNN) architecture.

- Step 3: PNN algorithm training. Input the traffic data with classification labels obtained in Step 2 into the PNN model for training. Then select a part as the test set to verify the model's accuracy.
- Step 4: Congestion category output.

5.3 | The SC-PNN algorithm performance simulation

5.3.1 | SC-PNN algorithm function simulation

To verify the functionality of the proposed algorithm, we generate a random set of test data sets. In the test data sets, each test data point contains information on three traffic parameters (road flow, queue length, and average road speed), and each traffic parameter takes values in the range [0:1].

Figure 16 shows the simulation results of the SC-PNN algorithm, which demonstrates the relationship between the traffic parameters. In Figure 16a, the traffic states are divided into five categories with clear boundaries, which shows that the algorithm can classify the data set well. In addition, the road queue length increases with the increase of traffic (Figure 16b), and the average road speed decreases with the rise of vehicle queue length (Figure 16c), which also satisfies the objective law.

5.3.2 | SC-PNN algorithm stability simulation

In order to better verify the performance of the proposed method, we graphically represent and compare the results of the traffic status labels obtained by the two algorithms over time (as shown in Figure 17).

In Figure 17, the abscissa represents time, the ordinate represents state classification, and numbers 1–5 represent the level of road congestion respectively: 1-very smooth, 2-smooth, 3-mild congestion, 4-congestion, and 5-severe congestion. The peak hours are 07:00–09:00, 11:00–12:00, and 17:00–18:00. The figure's red box indicates a difference in the discrimination between the two algorithms. The traffic state from 00:00 to 06:00 in Figure 17a is somewhat mistakenly divided into two states, but it has been classified as correct State 1 in Figure 17b. Some of the traffic states around 09:00–10:00 in Figure 17a are misclassified as state 5, but the state obtained after training with the PNN algorithm becomes state 4; in addition, 13:00–14:00 and after 18:00, there are misjudgment states, which are classified as correct traffic states after training by the PNN algorithm.

Through simulation verification, it can be obtained that the proposed SC-PNN algorithm can discriminate traffic congestion states. Compared with the individual SC algorithm, the state division is more accurate, and the anti-interference ability is stronger.

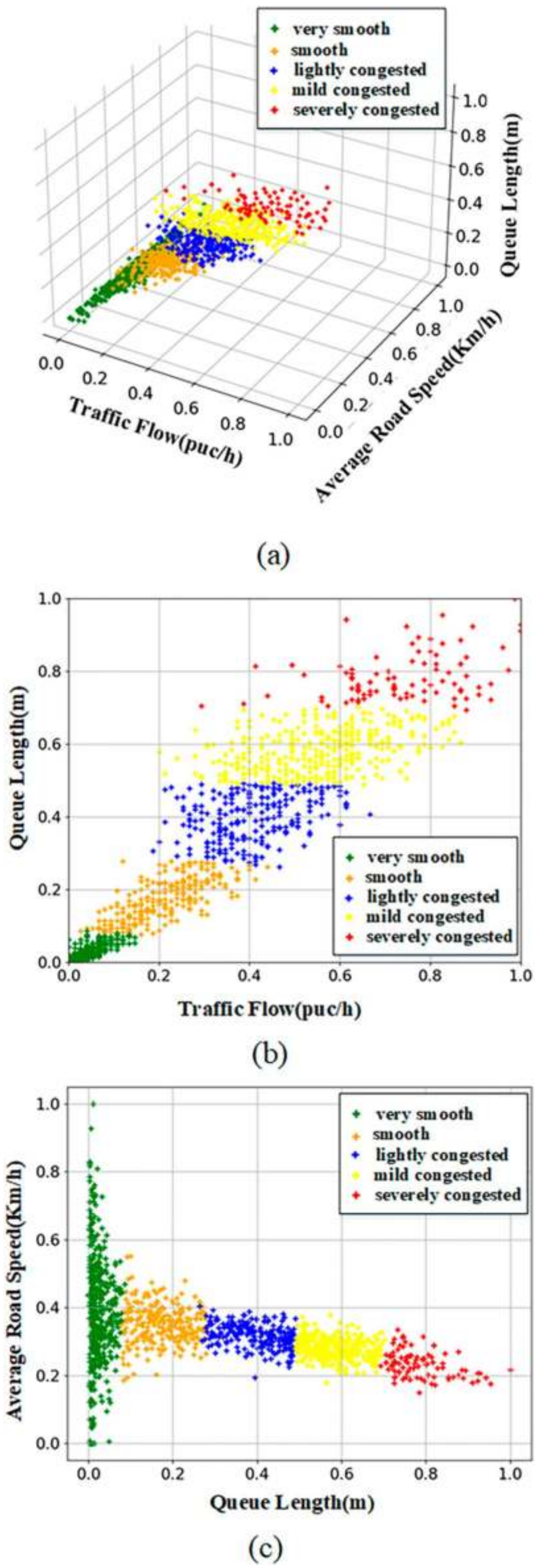

FIGURE 16 Traffic congestion state identification algorithm (the SC-PNN) function simulation. (a) The relationship between the traffic parameters in 3D view. (b) Simulation of the relationship between traffic flow and queue length. (c) Simulation of the relationship between queue length and average road speed.

6 | ACTUAL EXPERIMENTAL CASE AND RESULT ANALYSIS

The traffic congestion alleviation system was deployed at No. 191, Changshan Road, Laiyang City, Yantai City, Shandong Province, China. The system installation and the system's location are shown in Figure 18. Based on the actual road environment, we analyse the system's performance from two aspects, that is, counting the traffic parameter estimation accuracy and comparison of traffic congestion alleviation efficiency with the fixed-time traffic light system.

6.1 | Traffic parameter estimation results and analysis

The accuracy of traffic parameter estimation is an aspect that reflects the performance of the traffic congestion system. With 1 week (seven days) as the time interval, statistics of traffic parameters information at intersections are in multiple periods. In the performance analysis process, we use the traffic parameter results of manual statistics as the standard. The specific operation is, we installed video and speed-measuring devices on each road to achieving 24-h access to real vehicle information in the testing scenario. Then, the traffic flow is obtained by manually counting the number of vehicles at different periods in the recording. Simultaneously, they match the vehicles in the video with the speed information in the speed-measuring device to obtain the speed of each vehicle and the average road speed.

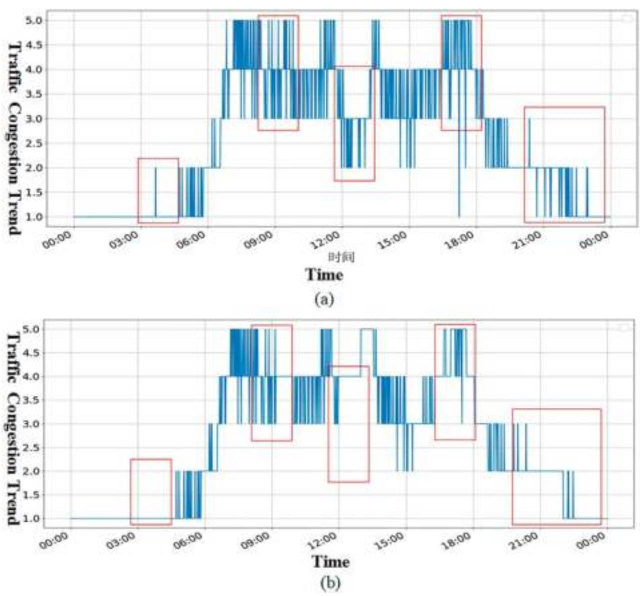

FIGURE 17 Traffic congestion state identification algorithm (the SC-PNN) stability simulation and comparison. (a) The spectral clustering (SC) algorithm traffic state-time trend. (b) The SC-PNN algorithm traffic state-time trend.

FIGURE 18 Traffic congestion alleviation system deployment.

6.1.1 | Road flow parameter estimation

The changes in traffic flow within a day are shown in Figure 19a. The flow reaches the maximum during the morning and evening peak hours, and the flow reaches the minimum at night. Figure 19b shows the difference between the estimated value of the model and the actual flow value during the period from 5 am to 9 am. When the flow rate is low, the relative error between the estimated and actual values is almost 0%. When the flow rate is high, the relative error between the estimated and true values does not exceed 15%.

6.1.2 | Road average speed parameter estimation

The changes in average road speed within a day are shown in Figure 20a. The average road speed is inversely proportional to traffic flow. At night or early in the morning, the road traffic flow is low, so the average road speed is zero or faster. During

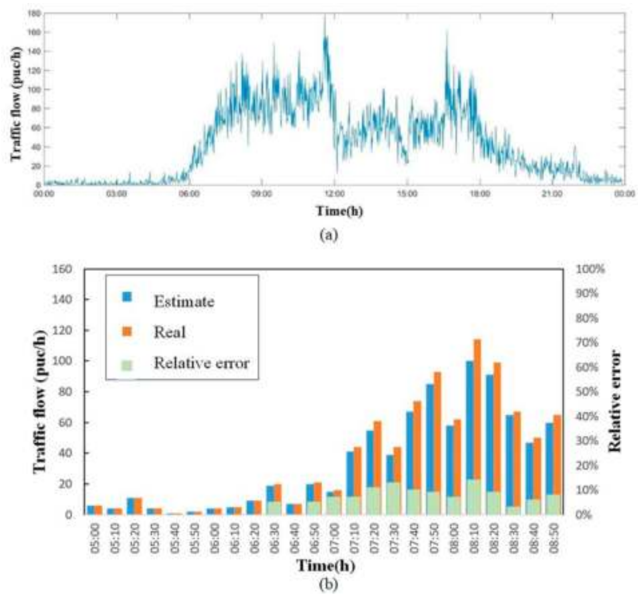

FIGURE 19 Traffic flow estimation and error analysis of traffic congestion alleviation system under real scenarios. (a) Traffic flow average estimation results in 1 day. (b) Comparison of traffic flow estimation results with real results.

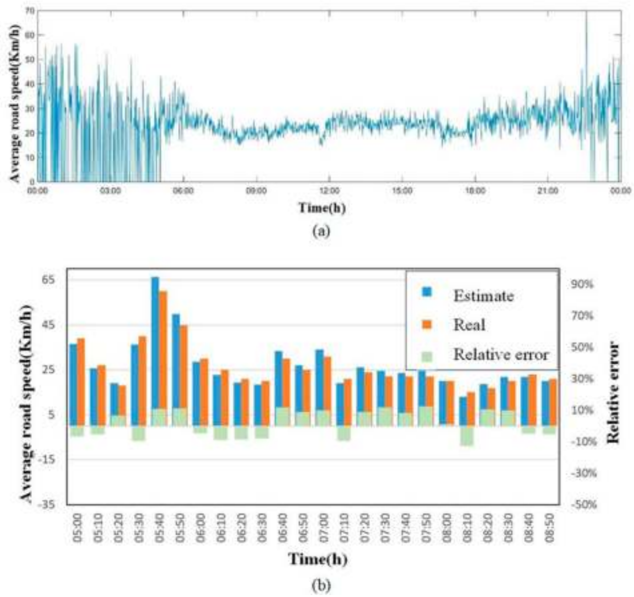

FIGURE 20 Road average speed estimation and error analysis of traffic congestion alleviation system under real scenarios. (a) Road average speed average estimation results in 1 day. (b) Comparison of road average speed estimation results with real results.

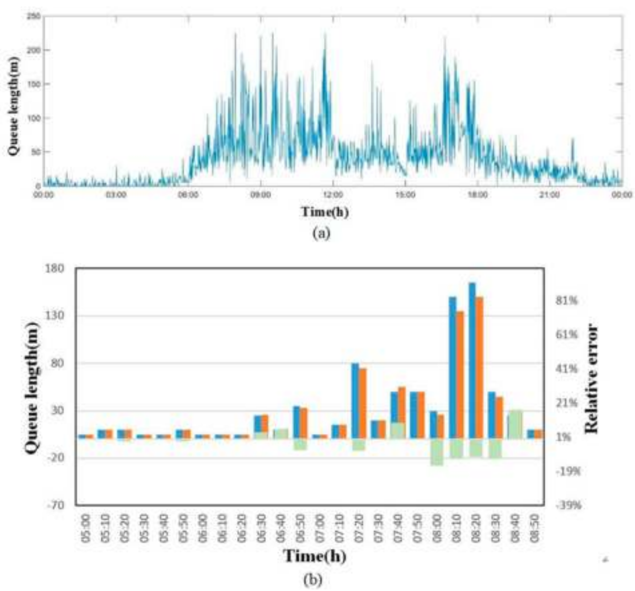

FIGURE 21 Road queue length estimation and error analysis of traffic congestion alleviation system under real scenarios. (a) Road queue length average estimation results in 1 day. (b) Comparison of Road queue length estimation results with real results.

the day, the speed of vehicles passing through the intersection does not exceed 40 Km/h, and the speed of vehicles generally decreases during peak hours. Figure 20b shows the difference between the estimated value of the model and the actual road average speed during the period from 5 am to 9 am. And the relative error between the estimated value of the average speed and the real value does not exceed 13%.

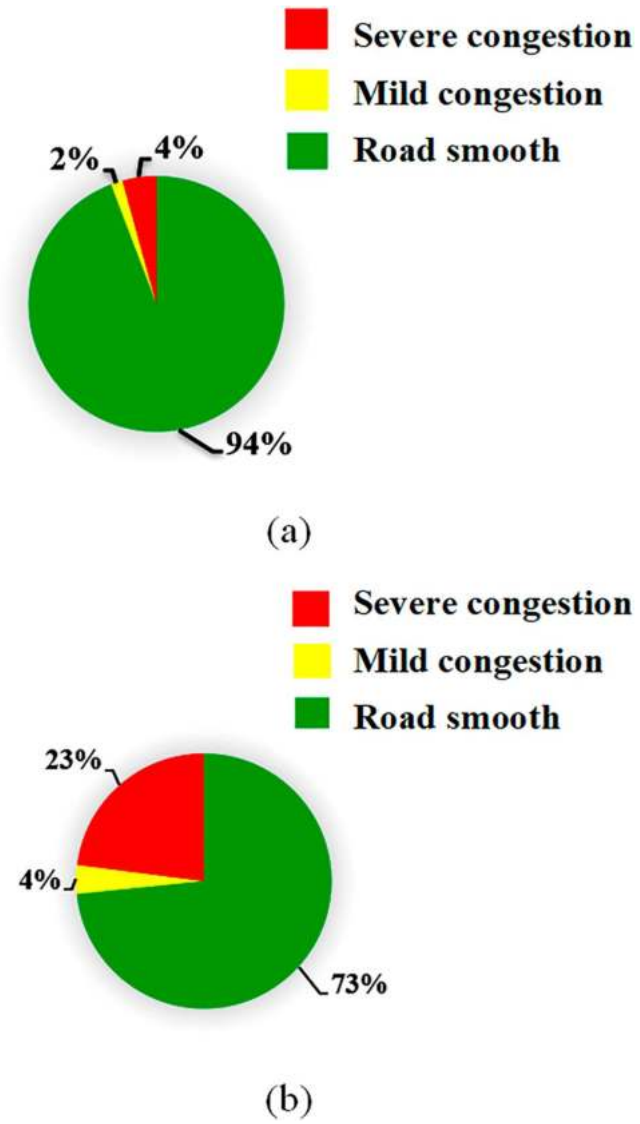

FIGURE 22 Average daily traffic congestion level ratio at intersections. (a) Traffic congestion alleviation system command result. (b) Fixed-time traffic light system command result.

6.1.3 | Road queue length parameter estimation

The changes in road queue length evaluation within a day are shown in Figure 21a. The road queue length is proportional to traffic flow. Figure 21b shows the difference between the estimated value of the model and the actual road queue length from 5 am to 9 am. When the road queue length is short, the relative error between the estimated and actual values is almost 0%. When the road queue length is long, the relative error between the estimated and actual values does not exceed 20%.

6.2 | Traffic congestion alleviation experiment

The most significant feature of this system solution is that it has been applied to actual intersections and achieved good

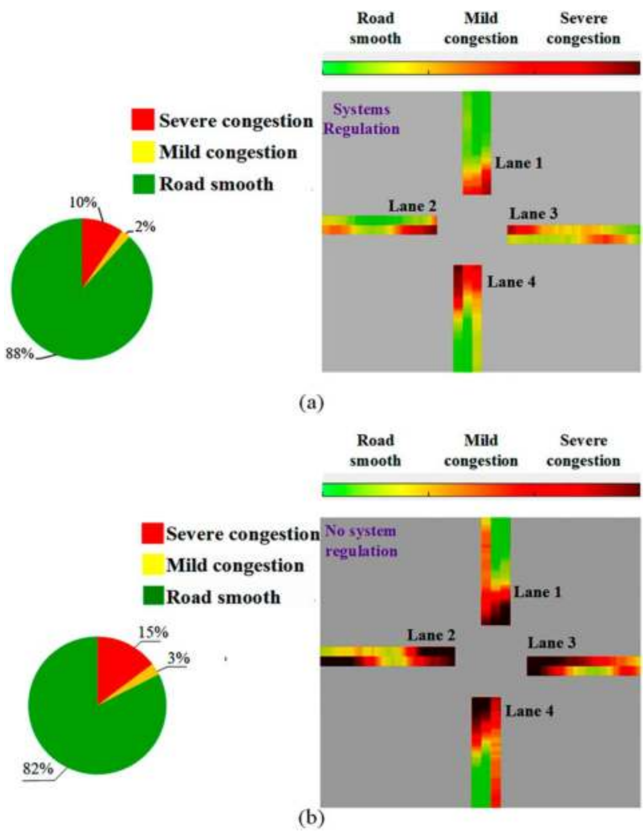

FIGURE 23 Average daily morning rush hour traffic congestion level ratio at intersections and lane status display. (a) Traffic congestion alleviation system command result. (b) Fixed-time traffic light system command result.

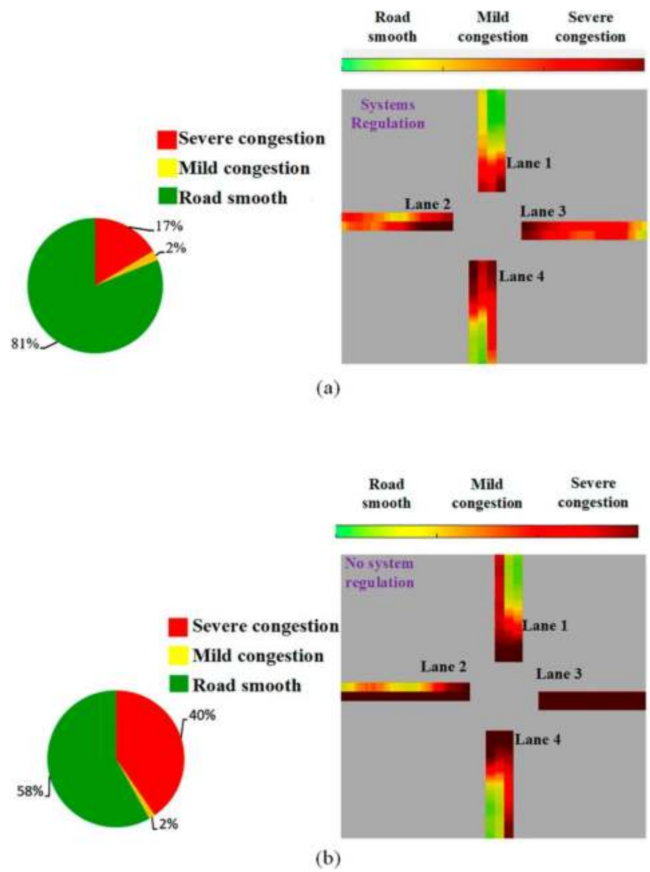

FIGURE 24 Average daily evening rush hour traffic congestion level ratio at intersections and lane status display. (a) Traffic congestion alleviation system command result. (b) Fixed-time traffic light system command result.

results by controlling the traffic lights to alleviate traffic congestion.

The traffic congestion alleviation system participates in the monitoring of traffic intersections and the control of traffic lights with 1 week as the time interval. When the radar traffic monitoring system is not involved, the original fixed-time traffic light system is adopted. Integrate the data in 1 week and perform the average processing on the data in multiple periods and finally get the traffic congestion information of the road in 1 day. Compare and record the road congestion under two methods.

To make the results more intuitive, the two results of very smooth and smooth are unified into smooth roads, and the congestion and severe congestion are unified into severe congestion. The final result is expressed in three states: smooth roads, mild congestion, and severe congestion. Figure 22 shows the proportion of traffic congestion at the intersection in 1 day after multiple time cycle statistics and processing. Under the command of the traffic congestion alleviation system, the proportion of road smooth has increased significantly, and the probability of severe congestion has decreased from 23% to 4%.

Figures 23 and 24 show the road traffic congestion during the morning and evening rush hours during the day. The picture on the left shows the proportion of different road conditions. The picture on the right shows the traffic situation of each lane when the congestion is the most serious. The deeper the red, the longer the queue length in the current lane and the more congested. Obviously, with the participation of the radar traffic system, the congestion rate in the morning peak and evening peak has been effectively alleviated by 20%.

7 | CONCLUSION

An urban traffic congestion alleviation system based on the millimeter-wave radar and an improved PNN is designed in this study. The system's architecture and data processing flow are introduced in detail, including the radar system for obtaining road vehicle driving information and the traffic congestion discrimination system for judging road congestion levels based on radar data. The system has been used in real urban intersections with good results rather than simulation: Compared to fixed traffic light control, the proposed road congestion alleviation system can effectively reduce the proportion of road congestion, especially the proportion of road congestion during peak hours by 20%. We hope that the system design can provide a reference for the application of radar in traffic command. In future work, we will implement control over multiple intersections, from single-intersection optimisation to regional optimisation.

AUTHOR CONTRIBUTIONS

Bo Yang: Writing—original draft. **Hua Zhang**: Writing—review & editing. **Mengxin Du**: Software. **Anna Wang**: Project administration. **Kai Xiong**: Project administration.

ACKNOWLEDGEMENTS

This work was supported partially by the Science and Technology on Near-Surface Detection Laboratory (No. 6142414211202), the Civil Aerospace Technology Advanced Research project (No. D020403) and the Basic Research project (No. 50236170112202). The authors greatly appreciate the above financial support.

CONFLICT OF INTEREST STATEMENT

This manuscript has not been published or presented elsewhere in part or in entirety and is not under consideration by another journal. There are no conflicts of interest to declare.

DATA AVAILABILITY STATEMENT

Author elects to not share data.

ORCID

Bo Yang https://orcid.org/0000-0001-6781-1850

REFERENCES

1. Ali, F., et al.: Traffic accident detection and condition analysis based on social networking data. Accid. Anal. Prev. 151, 105973 (2021). https://doi.org/10.1016/j.aap.2021.105973
2. Zhang, Y., et al.: A novel residual graph convolution deep learning model for short-term network-based traffic forecasting. Int. J. Geogr. Inf. Sci. 34(5), 969–995 (2020). https://doi.org/10.1080/13658816.2019.1697879
3. Ding, Q.Y., et al.: Forecasting traffic volume with space-time arima model. Adv. Mater. Res. 156, 979–983 (2011). https://doi.org/10.4028/www.scientific.net/amr.156-157.979
4. Guo, J., Huang, W., Williams, B.M.: Adaptive Kalman filter approach for stochastic short-term traffic flow rate prediction and uncertainty quantification. Transport. Res. C Emerg. Technol. 43, 50–64 (2014). https://doi.org/10.1016/j.trc.2014.02.006
5. Chen, P., et al.: Short-term traffic states forecasting considering spatial–temporal impact on an urban expressway. Transport. Res. Rec. 2594(1), 61–72 (2016). https://doi.org/10.3141/2594-10
6. Cai, P., et al.: A spatiotemporal correlative k-nearest neighbor model for short-term traffic multistep forecasting. Transport. Res. C Emerg. Technol. 62, 21–34 (2016). https://doi.org/10.1016/j.trc.2015.11.002
7. Feng, X., et al.: Adaptive multi-kernel SVM with spatial–temporal correlation for short-term traffic flow prediction. IEEE Trans. Intell. Transport. Syst. 20(6), 2001–2013 (2018). https://doi.org/10.1109/tits.2018.2854913
8. Kumar, K., Parida, M., Katiyar, V.: Short term traffic flow prediction for a non urban highway using artificial neural network. Proc. Soc. Behav. Sci. 104, 755–764 (2013). https://doi.org/10.1016/j.sbspro.2013.11.170
9. Li, Q., et al.: LSTM-based SQL injection detection method for intelligent transportation system. IEEE Trans. Veh. Technol. 68(5), 4182–4191 (2019). https://doi.org/10.1109/tvt.2019.2893675
10. Herrera-Quintero, L.F., et al.: Smart its sensor for the transportation planning based on iot approaches using serverless and microservices architecture. IEEE Intell. Transport. Syst. Mag. 10(2), 17–27 (2018). https://doi.org/10.1109/mits.2018.2806620
11. Li, L., et al.: Creditcoin: a privacy-preserving blockchain-based incentive announcement network for communications of smart vehicles. IEEE Trans. Intell. Transport. Syst. 19(7), 2204–2220 (2018). https://doi.org/10.1109/tits.2017.2777990
12. Tan, E., Chen, J.: Vehicular traffic density estimation via statistical methods with automated state learning. In: 2007 IEEE Conference on Advanced Video and Signal Based Surveillance, pp. 164–169. IEEE (2007)
13. Kim, D.H., et al.: Performance of vehicle speed estimation using wireless sensor networks: a region-based approach. J. Supercomput. 71(6), 2101–2120 (2015). https://doi.org/10.1007/s11227-014-1306-7
14. Balid, W., Tafish, H., Refai, H.H.: Intelligent vehicle counting and classification sensor for real-time traffic surveillance. IEEE Trans. Intell. Transport. Syst. 19(6), 1784–1794 (2017). https://doi.org/10.1109/tits.2017.2741507
15. Datondji, S.R.E., et al.: A survey of vision-based traffic monitoring of road intersections. IEEE Trans. Intell. Transport. Syst. 17(10), 2681–2698 (2016). https://doi.org/10.1109/tits.2016.2530146
16. Ganchimeg, G., Helmut, L.: Vision based vehicle monitoring at road intersections. In: 2018 International Conference on Electronics, Information, and Communication (ICEIC), pp. 1–4 (2018)
17. Abdelwahab, M.A., Abdel-Nasser, M., Taniguchi, R.I.: Efficient and fast traffic congestion classification based on video dynamics and deep residual network. In: International Workshop on Frontiers of Computer Vision, pp. 3–17. Springer (2020)
18. Gupta, S., et al.: A novel traffic surveillance system using an uncalibrated camera. J. Adv. Transport. 2022, 1–10 (2022). https://doi.org/10.1155/2022/5867524
19. Satyanarayana, G., Majhi, S., Das, S.K.: A vehicle detection technique using binary images for heterogeneous and lane-less traffic. IEEE Trans. Instrum. Meas. 70, 1–14 (2021). https://doi.org/10.1109/tim.2021.3062412
20. Mahmoud, M., Muradkhanli, L.: Economical and safe design for low-traffic long-roads illumination control system by using image recognition technique. J. Electr. Electron. Eng. 8(5), 117 (2020). https://doi.org/10.11648/j.jeee.20200805.11
21. Jia, Z.: Multi-target CFAR detection of a digital phased array radar system. J. Phys. Conf. 1314(1), 012011 (2019). https://doi.org/10.1088/1742-6596/1314/1/012011
22. Carretero, M.V., Harmanny, R.I.A., Trommel, R.P.: Smart-cfar, a machine learning approach to floating level detection in radar. In: 2019 16th European Radar Conference (EuRAD), pp. 161–164 (2019)
23. Zebiri, K., Mezache, A.: Radar cfar detection for multiple-targets situations for weibull and log-normal distributed clutter. Signal Image Video Process. 15, 1–8 (2021). https://doi.org/10.1007/s11760-021-01905-6
24. Zhou, H., Cao, P., Chen, S.: A novel waveform design for multi-target detection in automotive fmcw radar. In: 2016 IEEE Radar Conference (RadarConf), pp. 1–5 (2016)
25. Gonzalez, H., et al.: Doppler Ambiguity Resolution for Binary-Phase-Modulated Mimo Fmcw Radars, pp. 1–6 (2019)
26. Jeng, S.L., Chieng, W.H., Lu, H.P.: Estimating speed using a side-looking single-radar vehicle detector. IEEE Trans. Intell. Transport. Syst. 15(2), 607–614 (2014). https://doi.org/10.1109/tits.2013.2283528
27. Munoz-Ferreras, J.M., et al.: Traffic surveillance system based on a high-resolution radar. IEEE Trans. Geosci. Rem. Sens. 46(6), 1624–1633 (2008). https://doi.org/10.1109/tgrs.2008.916465
28. Xu, Y., Li, Y.: Improved velocity estimation algorithm for traffic surveillance radar using autofocus technique. Signal 2(2), 2 (2013)
29. Felguera-Martin, D., et al.: Vehicular traffic surveillance and road lane detection using radar interferometry. IEEE Trans. Veh. Technol. 61(3), 959–970 (2012). https://doi.org/10.1109/tvt.2012.2186323
30. Nishimura, K., Horiuchi, T., Yamada, H.: Target identification in traffic monitoring using millimeter-wave fm-cw radar. In: 2019 International Symposium on Antennas and Propagation (ISAP), pp. 1–2 (2019)
31. Park, J.-K., Choi, I.-O., Kim, K.-T.: Length prediction of moving vehicles using a commercial fmcw radar. IEEE Trans. Intell. Transport. Syst., 1–13 (2021)

32. Björklund, S.: Target detection and classification of small drones by boosting on radar micro-Doppler. In: 2018 15th European Radar Conference (EuRAD), pp. 182–185 (2018)
33. Ho, T.J., Chung, M.J.: An approach to traffic flow detection improvements of non-contact microwave radar detectors. In: 2016 International Conference on Applied System Innovation (ICASI), pp. 1–4 (2016)
34. Liu, H., et al.: Data feature analysis of non-scanning multi target millimeter-wave radar in traffic flow detection applications. Sensors 18(9), 2756 (2018). https://doi.org/10.3390/s18092756
35. Liu, S., Kawasaki, T., Zhai, Z.: Research on intersection phase timing calculating method based on interval detection data. In: Resilience and Sustainable Transportation Systems, pp. 109–117. American Society of Civil Engineers Reston, VA (2020)
36. Fu, Y., et al.: A camera–radar fusion method based on edge computing. In: 2020 IEEE International Conference on Edge Computing (EDGE), pp. 9–14. IEEE (2020)
37. Bai, J., et al.: Robust target detection and tracking algorithm based on roadside radar and camera. Sensors 21(4), 1116 (2021). https://doi.org/10.3390/s21041116
38. Xia, J., Chen, M.: A nested clustering technique for freeway operating condition classification. Comput. Aided Civ. Infrastruct. Eng. 22(6), 430–437 (2007). https://doi.org/10.1111/j.1467-8667.2007.00498.x
39. Zhu, G., Chen, J., Zhang, P.: Fuzzy c-means clustering identification method of urban road traffic state. In: 2015 12th International Conference on Fuzzy Systems and Knowledge Discovery (FSKD), pp. 302–307. IEEE (2015)
40. Pholsena, K., Pan, L.: Traffic status evaluation based on possibilistic fuzzy c-means clustering algorithm. In: 2018 IEEE Third International Conference on Data Science in Cyberspace (DSC), pp. 175–180. IEEE (2018)
41. Azimi, M., Zhang, Y.: Categorizing freeway flow conditions by using clustering methods. Transport. Res. Rec. 2173(1), 105–114 (2010). https://doi.org/10.3141/2173-13
42. Montazeri-Gh, M., Fotouhi, A.: Traffic condition recognition using the k-means clustering method. Sci. Iran. 18(4), 930–937 (2011). https://doi.org/10.1016/j.scient.2011.07.004
43. Li, H., et al.: Short-term passenger flow prediction under passenger flow control using a dynamic radial basis function network. Appl. Soft Comput. 83, 105620 (2019). https://doi.org/10.1016/j.asoc.2019.105620
44. Ata, A., et al.: Modelling smart road traffic congestion control system using machine learning techniques. Neural Netw. World 29(2), 99–110 (2019). https://doi.org/10.14311/nnw.2019.29.008
45. Niu, S., Liu, H.: Probabilistic neural networks for the identification of traffic state. In: 2011 14th International IEEE Conference on Intelligent Transportation Systems (ITSC), pp. 754–759. IEEE (2011)
46. Chen, B.H., Huang, S.C.: Probabilistic neural networks based moving vehicles extraction algorithm for intelligent traffic surveillance systems. Inf. Sci. 299, 283–295 (2015). https://doi.org/10.1016/j.ins.2014.12.033
47. Deng, C., et al.: Real-time freeway traffic state estimation based on cluster analysis and multiclass support vector machine. In: 2009 International Workshop on Intelligent Systems and Applications, pp. 1–4. IEEE (2009)
48. García, F.D.A., et al.: Ca-cfar detection performance in homogeneous weibull clutter. Geosci. Rem. Sens. Lett. IEEE 16(6), 887–891 (2018)
49. Finn, H.: Adaptive detection mode with threshold control as a function of spatially sampled clutter-level estimates. RCA Rev. 29, 414–465 (1968)
50. Rohling, H.: Radar cfar thresholding in clutter and multiple target situations. IEEE Trans. Aero. Electron. Syst. 4, 608–621 (1983). https://doi.org/10.1109/taes.1983.309350
51. Yang, B., Zhang, H.: A cfar algorithm based on Monte Carlo method for millimeter-wave radar road traffic target detection. Rem. Sens. 14(8), 1779 (2022). https://doi.org/10.3390/rs14081779
52. Schmidt, R.: Multiple emitter location and signal parameter estimation. IEEE Trans. Antenn. Propag. 34(3), 276–280 (1986). https://doi.org/10.1109/tap.1986.1143830
53. Roy, R., Kailath, T.: Esprit-estimation of signal parameters via rotational invariance techniques. IEEE Trans. Acoust. Speech Signal Process. 37(7), 984–995 (1989). https://doi.org/10.1109/29.32276
54. Cai, T.T., Wang, L.: Orthogonal matching pursuit for sparse signal recovery with noise. IEEE Trans. Inf. Theor. 57(7), 4680–4688 (2011). https://doi.org/10.1109/tit.2011.2146090
55. Yardibi, T., et al.: Source localization and sensing: a nonparametric iterative adaptive approach based on weighted least squares. IEEE Trans. Aero. Electron. Syst. 46(1), 425–443 (2010). https://doi.org/10.1109/taes.2010.5417172
56. Barton, P.: Digital beam forming for radar. In: IEE Proceedings F (Communications, Radar and Signal Processing), vol. 127, pp. 266–277. IET (1980)

How to cite this article: Yang, B., et al.: Urban traffic congestion alleviation system based on millimeter wave radar and improved probabilistic neural network. IET Radar Sonar Navig. 18(2), 327–343 (2024). https://doi.org/10.1049/rsn2.12443